ACI STRUCTURAL JOURNAL TECHNICAL PAPER

Title no. 100-S78

Design of Reinforced Concrete Solids Using Stress Analysis

by Stephen J. Foster, Peter Marti, and Nebojša Mojsilović

Linear finite element modeling of three-dimensional solid structures is well established, easy to apply, and readily available to designers. In the application of linear analysis in the design of concrete structures, however, it is not intuitive how to dimension the steel reinforcement to carry the stresses developed by the applied tractions. In this paper, a methodology for the design of reinforced concrete solid structures is presented using stress analysis combined with limit design. The admissible stress domain is presented in terms of Mohr's circles with solutions given for optimum reinforcement ratios, minimum concrete strength demand, and uniaxial concrete stress.

Keywords: design strength; reinforced concrete; stress.

INTRODUCTION

Today, most, if not all, structural engineering companies have access to a finite element (FE) package, although of varying degrees of sophistication. In fact, a number of public domain and shareware FE programs are available via the Web. Dimensioning of structures based on linear analyses of frames, as one example, is commonplace. Less common is the dimensioning of concrete plates, shells, and membrane type structures. Yet, it is in some of these structures where designers can benefit most by undertaking stress analyses. Some of the advantages of dimensioning based on linear FE modeling include:

- Linear FE modeling is well established and relatively easy to apply;
- Multiple load cases can be accommodated quickly; and
- The greatest quantity of reinforcement is placed in the high-tension regions helping to control crack propagation.

The main drawbacks in using the method are:

- No information is attained as to the collapse load of the structure (provided that ductility demands are met, designs based on elastic analyses will be safe for the limit design loads);
- No information is provided on inelastic phenomena such as crack widths, and crack spacing or deflections; and
- Detailing guidelines need to be established and followed to ensure ductility and serviceability demands are met.

The above aside, however, it is not always intuitive on how to dimension the reinforcing steel in two- and three-dimensional solids to meet the stress demands of the applied tractions obtained from an FE analysis. One method is to place adequate reinforcing steel in the direction of any principal tension stress and to ensure that the concrete has sufficient strength to meet all principal compressive stress demands. However, placing reinforcement in principal directions is not always convenient, and placement in the local structural or global directions is preferred. The question is then how to dimension reinforcement for any set of orthogonal axes for the six components of any applied stress tensor that define the stresses at a point. The answer to this question is presented in this paper.

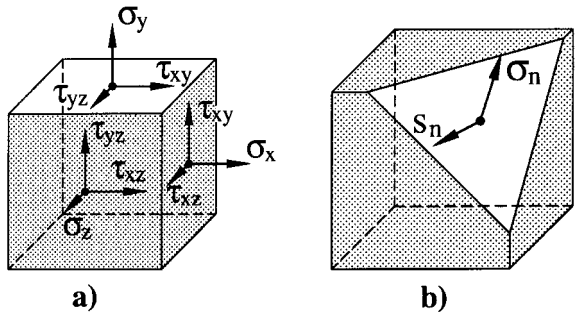

Fig. 1—Three-dimensional stresses: (a) orthogonal xyz *axis system; and (b) normal and shear stress for arbitrary plane.*

RESEARCH SIGNIFICANCE

Research, to date, on the use of linear stress analysis for the dimensioning of reinforced concrete structures has focused on the use of one- and two-dimensional elements such as frames, membranes, and slabs. In this research, a new and robust design process is developed for the dimensioning of reinforced concrete solids using linear stress analysis in combination with limit design. In addition to vast freedom in establishing suitable load paths in three dimensions, the paper gives the designer a tool for the calculation of stress rotations from the elastic precracked condition to the limit condition and, thus, provides the designer with the quantitative information necessary to make informed decisions on ductility demands of the structure. The methodology developed herein provides the designer with a valuable tool for the dimensioning of reinforced concrete solids.

BACKGROUND

In three-dimensional space, the stresses at a point are completely defined by the tensor

$$\sigma_{ij} = \begin{bmatrix} \sigma_x & \tau_{xy} & \tau_{xz} \\ \tau_{xy} & \sigma_y & \tau_{yz} \\ \tau_{xz} & \tau_{yz} & \sigma_z \end{bmatrix} \quad (1)$$

where *x, y, z* are any set of orthogonal axes, and the stresses are defined as shown in Fig. 1(a). Generally, a normal stress component is taken as positive if the component acts in a positive (negative) direction on an element face where a vector normal to the face is in a positive (negative) direction relative to the axis considered. The components are negative

ACI Structural Journal, V. 100, No. 6, November-December 2003.
MS No. 02-303 received August 14, 2002, and reviewed under Institute publication policies. Pertinent discussion including author's closure, if any, will be published in the September-October 2004 *ACI Structural Journal* if the discussion is received by May 1, 2004.

ACI member **Stephen J. Foster** *is an associate professor in the School of Civil and Environmental Engineering, University of New South Wales, Sydney, Australia. His research interests include the structural use of high-strength concretes, design of high-strength concrete columns, finite element modeling of reinforced concrete structures, and design of nonflexural members.*

ACI member **Peter Marti** *is a professor of structural engineering at the Institute of Structural Engineering, Swiss Federal Institute of Technology, Zurich, Switzerland. His research interests include the field of structural concrete.*

Nebojša Mojsilović *is a senior research associate and lecturer at the Institute of Structural Engineering at the Swiss Federal Institute of Technology. His research interests include structural masonry and concrete.*

if they act in a positive (negative) direction on an element face with a negative (positive) normal direction.

For every point in a body, there exist three stresses: $\sigma_{x'}$, $\sigma_{y'}$, and $\sigma_{z'}$ on the local $x'y'z'$ axis system such that $\tau_{x'y'} = \tau_{x'z'} = \tau_{y'z'} = 0$. These stresses are known as the principal stresses, and x', y', and z' are the principal axes. It is well established that the principal stresses are equal to the eigenvalues of the stress tensor. Perhaps less well recognized, however, is that the direction cosines to the principal axes are given by the norms of the eigenvectors of the stress tensor.

For any oblique plane (Fig. 1(b)) having a unit normal $\boldsymbol{n} = \{n_x, n_y, n_z\}$ passing through a point P, the stresses at P can be resolved into a component normal to the plane (σ_n) and a shear component parallel to the plane (S_n). For a stress to be principal, $S_n = 0$ which from Eq. (1) implies that

$$\begin{aligned} \sigma_x n_x + \tau_{xy} n_y + \tau_{xz} n_z &= \sigma_n n_x \\ \tau_{xy} n_x + \sigma_y n_y + \tau_{yz} n_z &= \sigma_n n_y \\ \tau_{xz} n_x + \tau_{yz} n_y + \sigma_z n_z &= \sigma_n n_z \end{aligned} \tag{2}$$

Rewriting Eq. (2) in the form $\boldsymbol{\sigma}.\boldsymbol{n} = 0$, it is seen that the equations are homogeneous. As all three components of $\boldsymbol{n}$ can not be zero, the solution is nontrivial only if the determinant of the coefficients $|\boldsymbol{\sigma}| = 0$, that is

$$\begin{vmatrix} \sigma_x - \sigma_n & \tau_{xy} & \tau_{xz} \\ \tau_{xy} & \sigma_y - \sigma_n & \tau_{yz} \\ \tau_{xz} & \tau_{yz} & \sigma_z - \sigma_n \end{vmatrix} = 0 \tag{3}$$

Expansion of Eq. (3) leads to the characteristic equation

$$\sigma_n^3 - I_1 \sigma_n^2 + I_2 \sigma_n - I_3 = 0 \tag{4}$$

where I_1, I_2, and I_3 are the invariants of the stress tensor given by

$$I_1 = \sigma_x + \sigma_y + \sigma_z = \sigma_1 + \sigma_2 + \sigma_3 \tag{5a}$$

$$I_2 = \sigma_x\sigma_y + \sigma_x\sigma_z + \sigma_y\sigma_z - (\tau_{xy}^2 + \tau_{xz}^2 + \tau_{yz}^2) \tag{5b}$$

$$= \sigma_1\sigma_2 + \sigma_1\sigma_3 + \sigma_2\sigma_3$$

$$I_3 = \sigma_x\sigma_y\sigma_z + 2\tau_{xy}\tau_{xz}\tau_{yz} - (\sigma_x\tau_{yz}^2 + \sigma_y\tau_{xz}^2 + \sigma_z\tau_{xy}^2) \tag{5c}$$

$$= \sigma_1\sigma_2\sigma_3$$

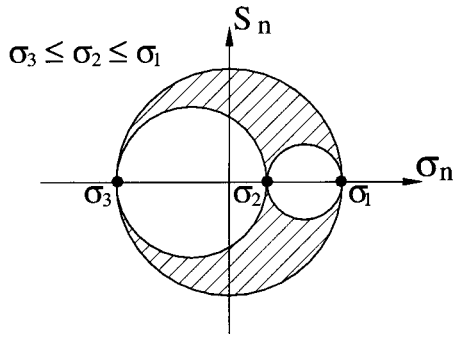

Fig. 2—Mohr's circles for stresses at point in three dimensions.

and where σ_1, σ_2, and σ_3 are the principal stresses. By common definition, the principal stresses are ordered such that $\sigma_3 \le \sigma_2 \le \sigma_1$. The principal stress directions $\boldsymbol{n_i} = \{n_{ix}, n_{iy}, n_{iz}\}(i = 1, 2, 3)$ are obtained from

$$n_{ix} = \frac{-c_{iy}c_{iz}}{C};\ n_{iy} = \frac{-c_{ix}c_{iz}}{C};\ n_{iz} = \frac{-c_{ix}c_{iy}}{C} \tag{6}$$

where $C = \sqrt{c_{ix}^2c_{iy}^2 + c_{ix}^2c_{iz}^2 + c_{iy}^2c_{iz}^2}$ and where

$$c_{ix} = (\sigma_x - \sigma_i)\tau_{yz} - \tau_{xy}\tau_{xz} \tag{7a}$$

$$c_{iy} = (\sigma_y - \sigma_i)\tau_{xz} - \tau_{xy}\tau_{yz} \tag{7b}$$

$$c_{iz} = (\sigma_z - \sigma_i)\tau_{xy} - \tau_{xz}\tau_{yz} \tag{7c}$$

Stresses at a point in three dimensions can be plotted in the form of Mohr's circles (Fig. 2) where the normal stress is plotted on the horizontal axis and the shear stress plotted on the vertical axis. Three principal circles are possible between the principal stress pairs $\sigma_1 - \sigma_2$, $\sigma_2 - \sigma_3$, and $\sigma_1 - \sigma_3$. In failure theorems, the principal stress pair 1 to 3 is regarded as the most important and the circle generated through this stress pair is referred to as the major principal stress circle.

In *xyz* space, σ_x, σ_y, and σ_z are, by definition, normal to the *yz*, *xz*, and *xy* planes, respectively. The magnitude of the shear stresses on these planes are given by

$$S_x = \sqrt{\tau_{xy}^2 + \tau_{xz}^2};\ S_y = \sqrt{\tau_{xy}^2 + \tau_{yz}^2};\ S_z = \sqrt{\tau_{xz}^2 + \tau_{yz}^2} \tag{8}$$

As the orientation of the *xyz* axis system is arbitrary, its interpretation represents all possible planes.

Once that the principal stresses have been found in magnitude and direction, the stresses on any oblique plane can be determined from

$$\sigma_n = \sigma_1 n_1^2 + \sigma_2 n_2^2 + \sigma_3 n_3^2 \tag{9a}$$

$$S_n^2 = \sigma_1^2 n_1^2 + \sigma_2^2 n_2^2 + \sigma_3^2 n_3^2 - \sigma_n^2 \tag{9b}$$

where n_i ($i = 1, 2, 3$) are the direction cosines relative to the principal axes of a vector normal to the plane. By noting the relationship between the direction cosines $n_1^2 + n_2^2 + n_3^2 = 1$, it can be shown for any fixed value of n_1 (eliminating n_2 and n_3 from Eq. (9b)) that

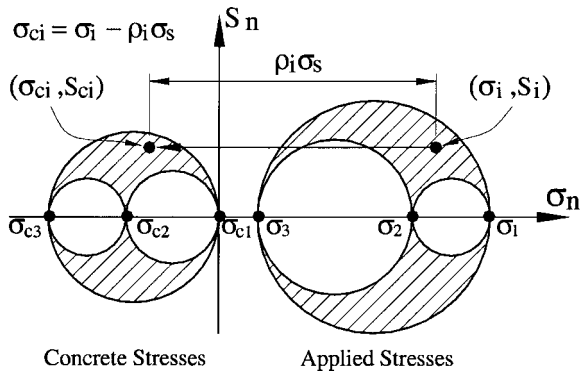

Fig. 3—Compression field for three-dimensional stress at point.

$$\left\{\sigma_n - \frac{1}{2}(\sigma_2 + \sigma_3)\right\}^2 + S_n^2 \tag{10a}$$

$$= n_1^2(\sigma_2 - \sigma_1)(\sigma_3 - \sigma_1) + \frac{1}{4}(\sigma_2 - \sigma_3)^2$$

and by permutation of subscripts

$$\left\{\sigma_n - \frac{1}{2}(\sigma_1 + \sigma_3)\right\}^2 + S_n^2 \tag{10b}$$

$$= n_2^2(\sigma_1 - \sigma_2)(\sigma_3 - \sigma_2) + \frac{1}{4}(\sigma_1 - \sigma_3)^2$$

$$\left\{\sigma_n - \frac{1}{2}(\sigma_1 + \sigma_2)\right\}^2 + S_n^2 \tag{10c}$$

$$= n_3^2(\sigma_1 - \sigma_3)(\sigma_2 - \sigma_3) + \frac{1}{4}(\sigma_1 - \sigma_2)^2$$

Mohr[1] observed that with $\sigma_3 \le \sigma_2 \le \sigma_1$, Eq. (10a) places the point (σ_n, S_n) on or outside the $\sigma_2 - \sigma_3$ circle and, similarly, Eq. (10b) places the point on or outside the $\sigma_1 - \sigma_2$ circle, and Eq. (10c) places it on or inside the $\sigma_1 - \sigma_3$ circle. Thus, the point (σ_n, S_n) lies within the hatched region of Fig. 2.

APPLICATION TO REINFORCED CONCRETE

Theory

In the applications that follow, the *xyz* axes are taken to correspond with reinforcing directions. The normal stresses applied at a point in a reinforced concrete solid element are carried by reinforcing steel and/or the concrete while shear stresses are carried by the concrete alone. Given that the applied stress tensor has been determined, for example, by three-dimensional finite element solid modeling, the Mohr's circles of applied stress can be plotted, as shown in Fig. 3. Within the circles, the stress points (σ_i, S_i) are also plotted where $i = x, y, z$. As the reinforcing steel can not carry shear stress, it follows that the points (σ_{ci}, S_{ci}) must fall within the hatched region of the concrete stress circles where $\sigma_{ci} = \sigma_i - \sigma_{si}$ and $S_{ci} = S_i$ and where σ_{si} are the equivalent steel stresses in the *i*-th direction.

Applying Eq. (1) to the stresses defined in Fig. 3, the tensor of the concrete stresses is written as

$$\sigma_{cij} = \begin{bmatrix} (\sigma_x - \sigma_{sx}) & \tau_{xy} & \tau_{xz} \\ \tau_{xy} & (\sigma_y - \sigma_{sy}) & \tau_{yz} \\ \tau_{xz} & \tau_{yz} & (\sigma_z - \sigma_{sz}) \end{bmatrix} \tag{11}$$

The equivalent reinforcement stresses are limited by

$$|\sigma_{sj}| \le \phi_t \rho_{sj} f_{yj} \tag{12}$$

where ρ_{sj} ($j = x, y, z$) are the reinforcement ratios in the *x*, *y*, and *z* directions, respectively; f_{yj} are the yield strengths of the reinforcement; and ϕ_t is a material reduction factor for tension elements.

With the convention $\sigma_{c3} \le \sigma_{c2} \le \sigma_{c1}$, the concrete stresses are required to satisfy

$$-\sigma_{c3} \le \beta\phi_c f_{cp} \tag{13}$$

where f_{cp} is the uniaxial strength of the in-place concrete (normally taken as $f_{cp} = 0.85f_c'$); β is a factor to account for triaxial effects on concrete strength (discussed in the section, Design Concrete Compression Strength); and ϕ_c is a material reduction factor for concrete.

The invariants of the concrete stress tensor are given by Eq. (5) with the appropriate substitutions for σ_x, σ_y, and σ_z. The principal directions of the applied stresses and those of the concrete stresses enclose angles δ_i ($i = 1, 2, 3$) and are given by

$$\delta_i = \cos^{-1}\left|n_{ix}n_{cix} + n_{iy}n_{ciy} + n_{iz}n_{ciz}\right| \tag{14}$$

where $\boldsymbol{n_{ci}}$ ($i = 1, 2, 3$) are the direction cosines of the concrete stress tensor.

Comparing Eq. (11) with Fig. 3, it is seen that there are five unknowns: σ_{c2}, σ_{c3}, σ_{sx}, σ_{sy}, and σ_{sz} (with $\sigma_{c1} = 0$ or another prescribed limit such as $\sigma_{c1} = \phi_c f_{ct}$ where f_{ct} is the concrete tension strength). As the solution to Eq. (3) provides for a maximum of three real roots, an infinity of solutions exist to Eq. (11). The designer has the freedom to apply two constraint equations with the three invariant equations making up the five equations required for a solution. The design process outlined above is demonstrated in the examples that follow.

Reinforcement dimensioning for three-dimensional stresses—Example 1

The results of a stress analysis on a concrete structural element give the stress tensor in the *xyz* axes as

$$\sigma_{ij} = \begin{bmatrix} 2 & 6 & -4 \\ 6 & -2 & 2 \\ -4 & 2 & 5 \end{bmatrix} \text{MPa} \tag{15}$$

It is desired to reinforce the element in the orthogonal directions of *xyz*. For the stresses defined by Eq. (15), the magnitudes of the shear stresses are $|S_x|$, $2\sqrt{13} \approx 7.21$ MPa, $|S_y| = 2\sqrt{10} \approx 6.32$ MPa, and $|S_z| = 2\sqrt{5} \approx 4.47$ MPa; and the principal stresses are $\sigma_1 = 8.28$ MPa, $\sigma_2 = 4.32$ MPa, and $\sigma_3 = -7.60$ MPa. The Mohr's circle of stress for the tensor of Eq. (15) is shown in Fig. 4(a). Viewing the stress plot

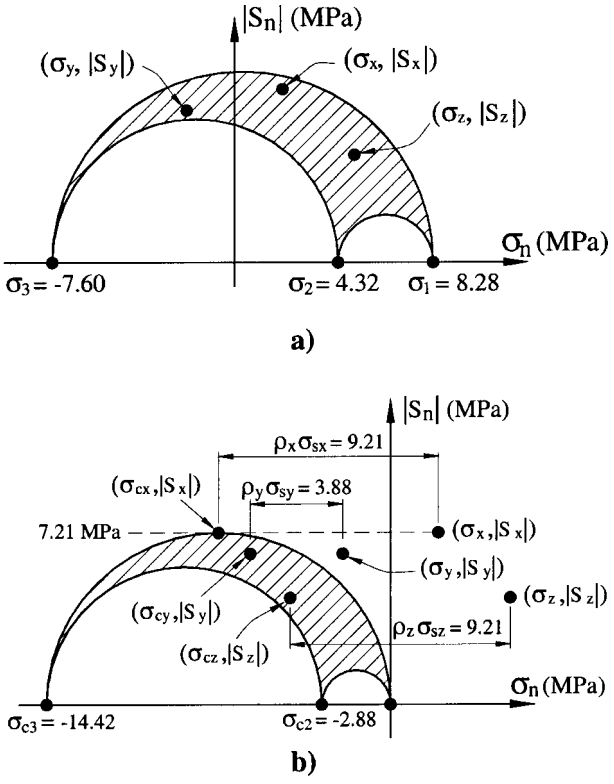

Fig. 4—Mohr's stress circles for Example 1: (a) applied stresses; and (b) concrete and reinforcement stresses.

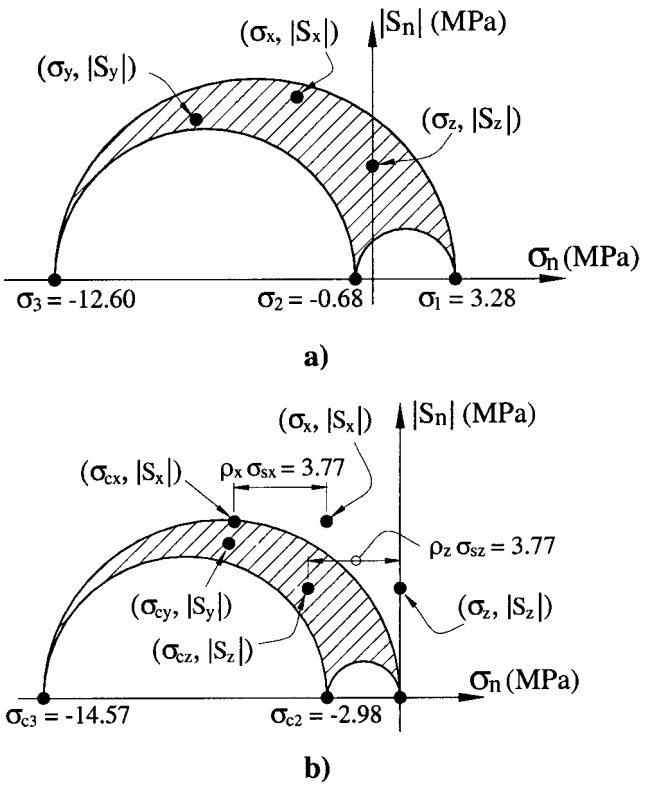

Fig. 5—Mohr's stress circles for Example 2: (a) applied stresses; and (b) concrete and reinforcement stresses.

(Fig. 4(a)), it is decided to seek the solution that gives the lowest demand on the concrete strength. This is established by selecting the smallest diameter for the major principal stress circle. As only the concrete carries shear stress the radius of the major stress circle (R_{1-3}) is constrained such that $R_{1-3} \geq \max(|S_x|, |S_y|, |S_z|)$, and thus, for this example, $R_{1-3} = |S_x| = 2\sqrt{3}$ MPa. Therefore, for the absolute minimum compression stress in the concrete, the constraint equations are given by

$$\sigma_{c3} = -2|S_x| = -4\sqrt{13} \text{ MPa} \quad (16a)$$

$$\rho_x f_{yd} = \sigma_x + |S_x| = 2 + 2\sqrt{13} \text{ MPa} \quad (16b)$$

where f_{yd} is the design strength of the reinforcement ($f_{yd} = \phi_t f_y$). Substituting Eq. (16a) and (16b) into the stress invariant equations given by Eq. (5a) to (5c), the following is written

$$I_1 \Rightarrow \sigma_{c2} - 4\sqrt{13} = 3 - 2\sqrt{13} - \rho_y f_{yd} - \rho_z f_{yd} \quad (17a)$$

$$I_2 \Rightarrow -4\sqrt{13}\sigma_{c2} = -2\sqrt{13}(3 - \rho_y f_{yd} - \rho_z f_{yd}) \quad (17b)$$

$$-(2 + \rho_y f_{yd})(5 - \rho_z f_{yd}) - 56$$

$$I_3 \Rightarrow 0 = 16\rho_y f_{yd} + 36\rho_z f_{yd} - 2\sqrt{13}(-2 - \rho_y f_{yd}) \quad (17c)$$

$$(5 - \rho_z f_{yd}) - 244 + 8\sqrt{13}$$

Solving Eq. (17a) to (17c) gives $\sigma_{c2} = -2.88$ MPa, $\rho_y f_{yd} = 3.88$ MPa, and $\rho_z f_{yd} = 9.21$ MPa. The final solution is plotted in Fig. 4(b).

Reinforcement dimensioning for three-dimensional stresses—Example 2

In the second example, the stress tensor is given

$$\sigma_{ij} = \begin{bmatrix} -3 & 6 & -4 \\ 6 & -7 & 2 \\ -4 & 2 & 0 \end{bmatrix} \text{ MPa} \quad (18)$$

and it is required to dimension the reinforcing steel. For the tensor of Eq. (18), the magnitude of the shears are $|S_x| = 7.21$ MPa, $|S_y| = 6.33$ MPa, and $|S_z| = 4.47$ MPa, and the principal stresses are $\sigma_1 = 3.28$ MPa, $\sigma_2 = -0.68$ MPa, and $\sigma_3 = -12.60$ MPa. The Mohr's circle of stress for the applied tractions is plotted in Fig. 5(a). After reviewing the stress circles, it is decided to seek a solution such that no reinforcing steel is required in the *y*-direction, that is, $\rho_y f_{yd} = 0$. Substituting this constraint into Eq. (5a) to (5c) gives

$$I_1 \Rightarrow \sigma_{c2} + \sigma_{c3} = -10 - \rho_x f_{yd} - \rho_z f_{yd} \quad (19a)$$

$$I_2 \Rightarrow \sigma_{c2}\sigma_{c3} = -35 + 7\rho_x f_{yd} + 10\rho_z f_{yd} + \rho_x\rho_z f_{yd}^2 \quad (19b)$$

$$I_3 \Rightarrow 0 = 28 + 4\rho_x f_{yd} + 15\rho_z f_{yd} - 7\rho_x\rho_z f_{yd}^2 \quad (19c)$$

Solutions to Eq. (19a) to (19c) are plotted in Fig. 6(a) and (b) for the intermediate principal concrete stress σ_{c2} versus the stress in the *x* and *z* reinforcement and for σ_{c2} versus σ_{c3}, respectively. Also plotted in Fig. 6(b) is σ_{c2} versus I_{c1}, where I_{c1} is the first invariant of stress given by the concrete stress circles (that is, $I_{c1} = \sigma_{c1} + \sigma_{c2} + \sigma_{c3}$). From the first stress invariant, it is seen that the minimum volume of reinforce-

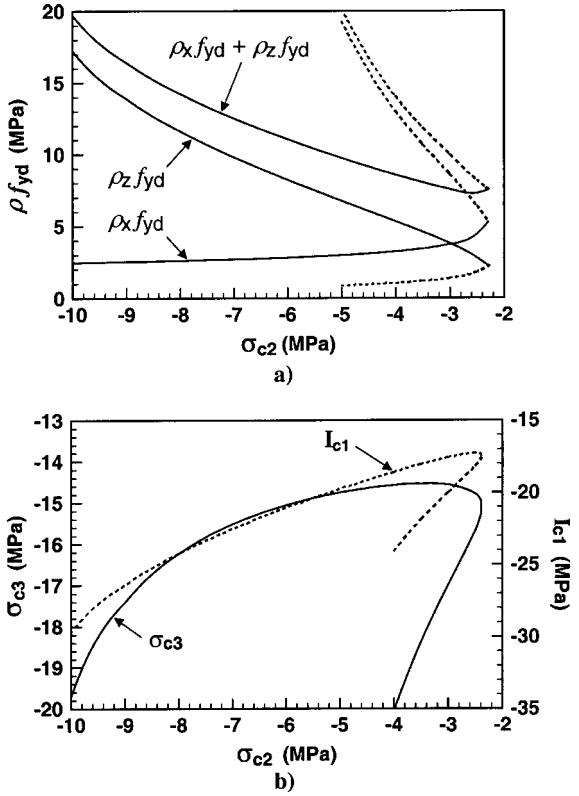

Fig. 6—Solutions to Eq. (19a) to (19c) for σ_{c2} versus: (a) reinforcement ratios; and (b) principal concrete stresses.

ment for a unit element with the stress tensor of Eq. (18) occurs at the point where I_{c1} is a maximum. In general, the optimal solutions lie at the upper end of σ_{c2}, as shown in Fig. 6(a) and (b) for the example at hand. After consideration, a solution is chosen such that $\rho_x f_{yd} = \rho_z f_{yd} = 3.77$ MPa, $\sigma_{c2} = -2.98$ MPa, and $\sigma_{c3} = -14.57$ MPa. The stress circles for the chosen solution are shown in Fig. 5(b).

GENERAL PROCEDURE FOR DIMENSIONING OF REINFORCEMENT

Theory

A general procedure can be developed for reinforcement dimensioning based on the principles developed previously.[2] For $\sigma_{c1} = 0$, the third invariant of the concrete stresses (Eq. (5c)) is $I_{c3} = 0$ and gives

$$\left(\sigma_{sx} - \sigma_x - \frac{\tau_{xz}^2}{\sigma_{sz} - \sigma_z}\right)\left(\sigma_{sy} - \sigma_y - \frac{\tau_{yz}^2}{\sigma_{sz} - \sigma_z}\right) = \left(\tau_{xy} + \frac{\tau_{xz}\tau_{yz}}{\sigma_{sz} - \sigma_z}\right)^2 \quad (20)$$

For any σ_{sz} = constant, Eq. (20) plots as the hyperbola shown in Fig. 7. By Eq. (20), any assumed or given σ_{sz} allows the determination of $\sigma_{sy}(\sigma_{sx})$ for any assumed $\sigma_{sx}(\sigma_{sy})$. Further, the no tension constraint ($\sigma_{c1} = 0$) dictates that, by Eq. (5b), for a solution to be valid

$$I_{c2} \geq 0 \quad (21)$$

A substitution of $I_{c3} = 0$ into Eq. (4) leads to

$$\sigma_{cn}^2 - I_{c1}\sigma_{cn} + I_{c2} = 0 \;\ldots.\; \{n = 2, 3\} \quad (22)$$

which has the roots

$$\sigma_{cn} = \frac{I_{c1}}{2} \pm \frac{1}{2}\sqrt{I_{c1}^2 - 4I_{c2}} \quad (23)$$

The first term of Eq. (23) ($I_{c1}/2$) defines the center of the 2 to 3 principal stress circle and the second term, the radius. The minor principal concrete stress σ_{c3} is obtained by taking the sign ahead of the square root term in Eq. (23) as negative, and the intermediate principal concrete stress σ_{c2} by taking the sign ahead of the square root term as positive. The concrete strength demand is then calculated by Eq. (13).

Uniaxial compression in concrete—For the limiting case of uniaxial compression in the concrete, the following is written: $\sigma_{c1} = \sigma_{c2} = 0$, $I_{c1} = \sigma_{c3}$, and $I_{c2} = I_{c3} = 0$. The solution to Eq. (20) is then characterized by

$$\sigma_{sx} = \sigma_x - \frac{\tau_{xy}\tau_{xz}}{\tau_{yz}}; \quad (24)$$

$$\sigma_{sy} = \sigma_y - \frac{\tau_{xy}\tau_{yz}}{\tau_{xz}};\ \sigma_{sz} = \sigma_z - \frac{\tau_{xz}\tau_{yz}}{\tau_{xz}}$$

and the required concrete strength is again obtained using Eq. (13).

Optimum reinforcement—For the purpose of definition in this paper, the optimum total reinforcement $\rho_x + \rho_y + \rho_z$ is taken as the minimum total volume of reinforcement for a unit element with the condition $\sigma_{sj} = \phi_t \rho_{sj} f_{yj} \geq 0$ ($j = x,y,z$). That is, all steel is in tension. For steel stresses of $f_{yj} = f_y$, $\rho_x + \rho_y + \rho_z$, is a minimum if $I_{c1} = I_1 - (\sigma_{sx} + \sigma_{sy} + \sigma_{sz})$ is a maximum. For any σ_{sz} = constant, this corresponds to Point A in Fig. 7 for which the sum $\sigma_{sx} + \sigma_{sy}$ is a minimum. Thus, using Eq. (20) the sum

$$\Sigma_z = \frac{\tau_{xz}^2 + \tau_{yz}^2}{\sigma_{sz} - \sigma_z} + 2\left|\tau_{xy} + \frac{\tau_{xz}\tau_{yz}}{\sigma_{sz} - \sigma_z}\right| + \sigma_{sz} - \sigma_z \quad (25)$$

must be minimized. Setting the derivative of Σ_z with respect to $\sigma_{sz} - \sigma_z$ equal to zero, one obtains

$$\sigma_{sz} = \sigma_z + |\tau_{xz} \pm \tau_{yz}| \quad (26a)$$

where the sign within the absolute term has to be chosen such that Σ_z is minimized. Substituting $\sigma_{sz} - \sigma_z$ from Eq. (26a) into the expression for the coordinates of Point A in Fig. 7, the analogous requirements

$$\sigma_{sx} = \sigma_x + |\tau_{xy} \pm \tau_{xz}| \quad (26b)$$

$$\sigma_{sy} = \sigma_y + |\tau_{xy} \pm \tau_{yz}| \quad (26c)$$

are obtained for optimum reinforcement.

Reinforcement dimensioning for three-dimensional stresses—Example 3

Consider again the stress tensor given by Eq. (15) with the principal stresses of $\sigma_1 = 8.28$ MPa, $\sigma_2 = 4.32$ MPa, and $\sigma_3 = -7.60$ MPa. The direction cosines for the principal stress

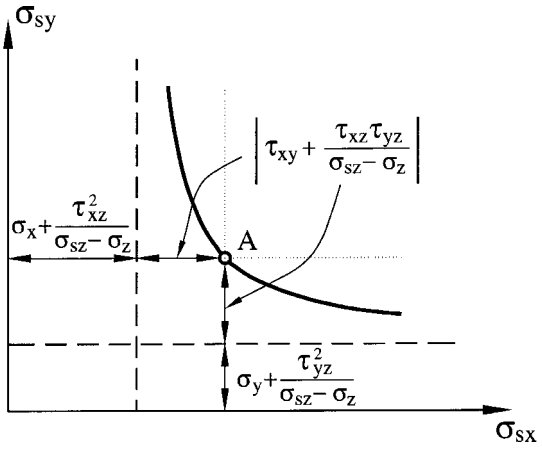

Fig. 7—Equivalent stresses in reinforcement for σ_{sz} = constant.

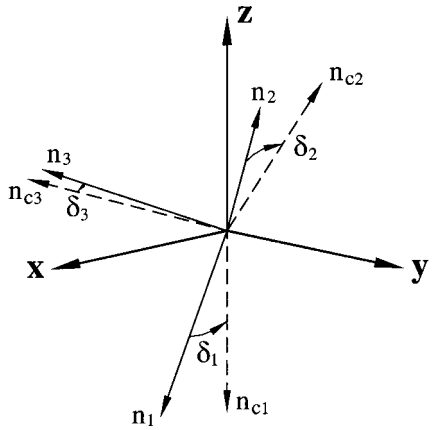

Fig. 8—Comparison of concrete principal stress directions and principal directions due to applied tractions for case of optimum reinforcement.

directions $\boldsymbol{n_i}$ are obtained by Eq. (6) and (7) and are $\boldsymbol{n_1}$ = {0.688, 0.270, –0.674}, $\boldsymbol{n_2}$ = {0.419, 0.610, 0.672}, and $\boldsymbol{n_3}$ = {0.593, –0.745, 0.306}.

Optimum reinforcement solution—For a positive sign within the absolute term on the right-hand side of Eq. (26a), $\sigma_{sx} - \sigma_x = 2$ MPa is obtained and the sum given by Eq. (25a) is $\Sigma_x = 48$ MPa. Taking a negative sign within the absolute term gives $\sigma_{sx} - \sigma_x = 10$ MPa and the sum amounts to Σ_x = 16 MPa. Thus, in the *x*-direction, the negative sign governs and $\sigma_{sx} - \sigma_x = 10$ MPa. Similarly, in the *y*- and *z*-directions, the negative and positive signs govern in Eq. (26b) and (26c), respectively, and $\sigma_{sy} - \sigma_y = 4$ MPa and $\sigma_{sz} - \sigma_z = 2$ MPa.

With the components of $\sigma_{si} - \sigma_i$ ($i = x, y, z$) determined, the concrete stress tensor is now calculated by Eq. (11) and is

$$\sigma_{cij} = \begin{bmatrix} -10 & 6 & -4 \\ 6 & -4 & 2 \\ -4 & 2 & -2 \end{bmatrix} \text{ MPa} \qquad (27)$$

and then by Eq. (6)

$$\boldsymbol{n_{c1}} = \{0.577, 0.577, 0.577\} \qquad (28a)$$

$$\boldsymbol{n_{c2}} = \{0.099, 0.653, 0.751\} \qquad (28b)$$

$$\boldsymbol{n_{c3}} = \{0.810, -0.491, 0.320\} \qquad (28c)$$

The principal directions of the applied stresses are compared with the directions of the concrete stresses by Eq. (14) giving δ_1 = 19.6 degrees, δ_2 = 19.1 degrees, and δ_3 = 19.3 degrees, which are plotted in Fig. 8.

A check on the second invariant of the concrete stress tensor of Eq. (27) shows that $I_{c2} = 12$ MPa$^2 \geq 0$ and, therefore, by Eq. (21) the solution is judged valid. With $I_{c1} = -16$ MPa, the concrete strength demand is obtained from Eq. (23) and is $\sigma_{c3} = -15.21$ MPa and the specified concrete strength obtained by the application of Eq. (13). The intermediate principal concrete stress is $\sigma_{c2} = -0.79$ MPa.

Uniaxial compression in concrete solution—Substitution of the tensor given by Eq. (15) into Eq. (24) results in σ_{sx} = 14 MPa, $\sigma_{sy} = 1$ MPa, and $\sigma_{sz} = 6.33$ MPa. The concrete stress tensor is again determined with Eq. (11) and is

$$\sigma_{cij} = \begin{bmatrix} -12 & 6 & -4 \\ 6 & -3 & 2 \\ -4 & 2 & -1.33 \end{bmatrix} \text{ MPa} \qquad (29)$$

The concrete strength demand is obtained by summing the diagonal terms of Eq. (29), that is, $\sigma_{c3} = -16.33$ MPa. The application of Eq. (6) yields $\boldsymbol{n_{c3}}$ = {0.857, –0.429, 0.286}, and from Eq. (14), $\delta_1 = 16.3$ degrees, $\delta_2 = 16.8$ degrees, and $\delta_3 = 23.8$ degrees. By comparison with the optimum reinforcement solution $\rho_x + \rho_y + \rho_z$ is increased by 1.6%, δ_3 is increased by 4.5 degrees, but δ_1 and δ_2 are decreased by 3.3 degrees and 2.3 degrees, respectively.

TWO-DIMENSIONAL STRESS ANALYSIS

In the case where one of the three global axes is aligned with a principal axis, as is the case for plane stress and plane strain, then the shear stresses associated with the axis are zero. For the purpose of discussion, the authors aligned the global *z*-axis with the principal 2-axis and removed the order constraint with reference to σ_2 but maintained the convention for σ_1 and σ_3. That is, $\sigma_1 \geq \sigma_3$ but $\sigma_2 \geq$ or $\leq \sigma_1, \sigma_3$. Considering only planes normal to the 2-axis (that is, $n_2 = 0$), then from Eq. (10b) the following is obtained

$$\left\{\sigma_n - \frac{\sigma_1 + \sigma_3}{2}\right\}^2 + S_n^2 = \left\{\frac{\sigma_1 - \sigma_3}{2}\right\}^2 \qquad (30)$$

Equation (30) is in the familiar form of $(x - a)^2 + y^2 = b^2$ and is the equation of the 1 to 3 stress circle centered at $a = (\sigma_1 + \sigma_3)/2$ and of radius $b = (\sigma_1 - \sigma_3)/2$. Thus, for plane stress and plane strain, all solutions lie on the boundary of the 1 to 3 stress circle. Similar expressions to that of Eq. (30) can be derived for the case where any of the global stress axes are aligned with any of the principal stress axes. In general, when one of the global axes is aligned such that it is also a principal axis, then all solutions for planes normal to this axis must lie on the boundary of the stress circle not associated with the axis.

For the particular case of plane stress, the relationships developed in this paper for dimensioning of reinforced concrete solids degenerate to the well-established dimensioning rules and yield criteria for membranes (References 3 to 8).

GENERAL COMMENTS

Concrete stress angles δ_i

In developing solutions using linear analysis, the designer must respect the limitations of the concrete material. In a solid subject to a constant ratio of normal and shear stresses (with at least one tensile principal stress) before cracking, the stress field in the concrete remains relatively elastic and the stresses in the reinforcement are negligible. After cracking, the tension stresses in the concrete reduce while those in the reinforcing steel increase. If the concrete does not fail in compression, then the crack directions will remain relatively stable until yield of the steel in one direction. After yield in one direction, the forces are continuously redistributed to balance the applied tractions until yield in all directions has occurred. Concrete elements such as panels, for example, have a limit on the amount of redistribution that can be achieved. As a rule, concrete elements should not be pushed far beyond that which is natural. Designers must critically examine the load path being assumed to satisfy themselves that a sufficient level of ductility is available to meet the demands of the imposed tractions. As a tentative recommendation, the authors suggest a limit of 25 degrees to δ_i. Further research is required, however, to corroborate this statement.

Design concrete compression strength

The factor β given in Eq. (13) accounts for both confinement effects, as is the case for concrete in biaxial or triaxial compression, and disturbance effects such as caused by the transmission of tension fields through compression fields. It has been shown by a number of researchers[9-14] that the disturbing effect of passing tension reinforcement through concrete in compression weakens the concrete. In addition, as concrete strength is increased, the concrete becomes more brittle. To account for the imperfect assumption that concrete behaves as a rigid-plastic material and to make sure that the ductility demands can be met, an efficiency factor is introduced to ensure that the concrete is not overstressed.

While there are a number of variants of the efficiency factor relationship, the model by Collins and Mitchell[15] has generally withstood the test of time. Based on the panel tests of Vecchio and Collins,[10,11] Collins and Mitchell proposed that

$$\beta = \frac{1}{0.8 + 170\varepsilon_1} \leq 1.0 \qquad (31)$$

where ε_1 is the major principal strain normal to the direction of the compression field. The transverse strain is required to be sufficiently large for the ductility demand to be met. Adopting ε_1 of 0.005 (twice the yield strain of steel for f_y = 500 MPa) gives $\beta = 0.6$.

Not all members or subelements of members, however, are subject to significant transverse strains, and a reduction to the degree of $\beta = 0.6$ is unjustified. For the case where transverse strains are small and the concrete is essentially in uniaxial or biaxial compression, the concrete is undisturbed by crossing tension stress fields. As a guide, if the major principal stress due to the applied loads is such that $\sigma_1 < 0.33\sqrt{f_c'}$ (in MPa), then the disturbance factor may be taken as $\beta = 1.0$. For concrete in triaxial compression, β may be determined using an appropriate triaxial stress model.

CONCLUSIONS

Linear finite element modeling of three-dimensional solid structures is well established, easy to apply, and readily available to designers. In the application of linear analysis in the design of concrete structures, however, how to dimension the steel reinforcement to carry the stresses developed due to applied tractions is not necessarily obvious or intuitive. In this paper, a methodology for the design of reinforced concrete solid structures is presented using stress analysis combined with limit design. The admissible stress domain is presented in terms of Mohr's circles with two-dimensional membrane structures noted as a special case of three-dimensional solids.

Limit design is a powerful tool for the dimensioning of reinforced concrete structures with its foundations in the lower-bound method of the theory of plasticity. Provided that sufficient ductility exists in the structure, the designer may provide any one of an infinity of statically admissible stress fields that satisfy the applied tractions. A method is given for the determination of the rotations of the concrete stress angles from those of the linear-elastic solution, and limitations on these rotations have been discussed.

ACKNOWLEDGMENTS

The work reported in this study was undertaken while the first author was on study leave at the Institute of Structural Engineering, the Swiss Federal Institute of Technology, Zürich, Switzerland. The assistance of the staff of the Institute and the provision by the Institute of the resources necessary to complete this work are gratefully acknowledged.

REFERENCES

1. Mohr, O., *Abhandlungen aus dem Gebiete der technischen Mechanik*, 2nd Edition, W. Ernst and Son, 1914, pp. 192-235.

2. Marti, P.; Mojsilovic, N.; and Foster, S. J., "Dimensioning of Orthogonally Reinforced Concrete Solids," *Structural Concrete in Switzerland*, *fib*-CH, *fib*-Congress, Osaka, Japan, Oct. 13-19, 2002, pp. 18-23.

3. Nielsen, M. P., "Yield Conditions for Reinforced Concrete Shells in the Membrane State," *Non-Classical Shell Problems*, Proceedings of the IASS Symposium, Warsaw, Poland, Sept. 2-5, 1964, pp. 1030-1040.

4. Nielsen, M. P., "On the Strength of Reinforced Concrete Discs," *Civil Engineering and Building Construction Series* 70, Acta Polytechnica Scandinavica, Copenhagen, 1971, 261 pp.

5. Müller, P., *Plastische Berechnung von Stahlbetonscheiben und -balken*, Institut für Baustatik und Konstruktion, ETH Zürich, Bericht Nr. 83, July 1978, 160 pp.

6. Morley, C. T., "Yield Criteria for Elements of Reinforced Concrete Slabs," *IABSE Report*, IABSE Colloquium on Plasticity in Reinforced Concrete, Copenhagen, V. 28, May 21-23, 1979, pp. 35-47.

7. Marti, P., "Plastic Analysis of Reinforced Concrete Shear Walls," *IABSE Report*, IABSE Colloquium on Plasticity in Reinforced Concrete, Copenhagen, V. 28, May 21-23, 1979, pp. 51-69.

8. Marti, P., "Dimensioning and Detailing," *IABSE Report*, IABSE Colloquium on Structural Concrete, Stuttgart, V. 62, Apr. 10-12, 1991, pp. 411-443.

9. Robinson, J. R., and Demorieux J.-M., "Essais de modéles d'âme de poutre en double té," *Annales de l'Institut Technique du Bâtiment et des Travaux Publics*, No. 354, Série: Béton 172, Oct. 1977, pp. 77-95.

10. Vecchio, F. J., and Collins, M. P, "The Response of Reinforced Concrete to In-Plane Shear and Normal Stresses," *Report* No. 82-03, Department of Civil Engineering, University of Toronto, Ontario, Canada, Mar. 1982, 332 pp.

11. Vecchio, F. J., and Collins, M. P., "The Modified Compression Field Theory for Reinforced Concrete Elements Subjected to Shear," ACI JOURNAL, *Proceedings* V. 83, No. 2, Mar.-Apr. 1986, pp. 219-231.

12. Miyakawa, T.; Kawakami, T.; and Maekawa, K., "Nonlinear Behavior of Cracked Concrete Reinforced Concrete Plate Element under Uniaxial Compression," *Proceedings of the JSCE*, No. 378, Aug. 1987, pp. 249-258.

13. Belarbi, A., and Hsu, T. T. C., "Constitutive Laws of Reinforced Concrete in Biaxial Tension Compression," *Research Report* UHCEE 91-2, Department of Civil Engineering, University of Houston, Houston, Tex., 1991, 155 pp.

14. Pang, X. B., and Hsu, T. T. C., "Constitutive Laws of Reinforced Concrete in Shear," *Research Report* UHCEE92-1, Department of Civil Engineering, University of Houston, Houston, Tex., 1992, 188 pp.

15. Collins, M. P., and Mitchell, D., "Rational Approach to Shear Design—The 1984 Canadian Code Provisions," ACI JOURNAL, *Proceedings* V. 83, No. 6, Nov.-Dec. 1986, pp. 925-933.